*sustainability*

MDPI

*Article*

# Internal Force Mechanism of Pisha Sandstone as a Soil Amendment to Improve Sandy Soil Structural Stability in Mu Us Sandy Land

**Zhe Liu [1,2,3], Lin Zhou [4], Yang Zhang [1,2,3,*], Jichang Han [1,2,3], Yingying Sun [1,2,3], Ruiqing Zhang [1,2,3], Xuxiang Li [1] and Feinan Hu [4,*]**

[1] Technology Innovation Center for Land Engineering and Human Settlements, Shaanxi Land Engineering Construction Group Co., Ltd. and Xi'an Jiaotong University, School of Human Settlements and Civil Engineering, Xi'an Jiaotong University, Xi'an 710049, China; liuzhe168@stu.xjtu.edu.cn (Z.L.); hanjc_sxdj@126.com (J.H.); sunyy526@163.com (Y.S.); zhangruiq2010000@163.com (R.Z.); xxli@mail.xjtu.edu.cn (X.L.)

[2] Shaanxi Provincial Land Engineering Construction Group Co., Ltd., Xi'an 710075, China

[3] Institute of Land Engineering and Technology, Shaanxi Provincial Land Engineering Construction Group Co., Ltd., Xi'an 710075, China

[4] State Key Laboratory of Soil Erosion and Dryland Farming on the Loess Plateau, Institute of Soil and Water Conservation, Chinese Academy of Sciences and Ministry of Water Resources, Yangling, Xianyang 712100, China; zhoulin@nwafu.edu.cn

* Correspondence: zhangyang_dj@163.com (Y.Z.); hufn@nwafu.edu.cn (F.H.); Tel./Fax: +86-29-8662-5019 (Y.Z. & F.H.)

**Abstract:** Compounding Pisha sandstone (PSS) with sandy soil in Mu Us Sandy Land is a viable agronomical measure to effectively reduce soil erosion and improve soil quality due to the complementary characters and structures of the two materials. Aggregate stability is an important indicator to assess sandy soil erosion resistance and quality, which could be largely affected by soil surface electrochemical properties and particle interaction forces. However, the effect of the compound ratio and particle interaction forces on the aggregate stability of compound soils with Pisha sandstone and sandy soil is still unclear. Therefore, in this study, the electrochemical properties, particle interaction forces, and their effects on the aggregate stability of PSS and sandy soil at five volume ratios (0:1, 1:5, 1:2, 1:1, and 1:0) were determined to clarify the internal force mechanism of PSS to increase sandy soil structural stability in a 10-year field experiment. Experiments were measured by a combined method for the determination of surface properties and aggregate water stability. A ten-year field study revealed that the incorporation of Pisha sandstone significantly enhanced the soil organic carbon (SOC) and cation exchange capacity (CEC) ($p < 0.05$), while the CEC value notably increased from 4.68 to 13.76 cmol·kg$^{-1}$ ($p < 0.05$). The soil surface potential (absolute value) and the electric field intensity gradually decreased with the increase in the Pisha sandstone content. For the compound soil particle interaction force, the addition of Pisha sandstone enhanced the van der Waals attraction force, reduced the net repulsive force between compound soil particles, and promoted the agglomeration of aeolian sandy soil. The overall trend of the aggregate breaking strength of compound soils under different addition ratios of PSS was 1:0 > 1:1 > 0:1 > 1:5 > 1:2. When the Pisha sandstone content in the compound soils was <50%, the aggregate stability was mainly influenced by compound soil particle interaction forces, and the interaction force increase was the key reason for the aggregate breakdown. When the Pisha sandstone content in the compound soils was ≥50%, the aggregate stability was affected by the combined effects of the compound soil particle composition and particle interaction forces. These results indicate that PSS addition ratios and particle interaction force are important factors affecting the structural stability of compound soils, in which the volume ratio of PSS to sandy soil of 1:2 is the appropriate ratio. Our study provides some theoretical references for further understanding of the compound soil structure improvement and sandy soil erosion control in Mu Us Sandy Land.



**Citation:** Liu, Z.; Zhou, L.; Zhang, Y.; Han, J.; Sun, Y.; Zhang, R.; Li, X.; Hu, F. Internal Force Mechanism of Pisha Sandstone as a Soil Amendment to Improve Sandy Soil Structural Stability in Mu Us Sandy Land. *Sustainability* **2024**, *16*, 4415. https://doi.org/10.3390/su16114415

Academic Editor: Eleftherios Evangelou

Received: 14 April 2024
Revised: 9 May 2024
Accepted: 21 May 2024
Published: 23 May 2024

**Keywords:** Pisha sandstone; compound soil; electrochemical properties; aggregate structural stability; particle interaction; Mu Us Sandy Land

## 1. Introduction

Mu Us Sandy Land, one of China's four major sandy lands, is in the southeastern part of Inner Mongolia and the northern loess Plateau of Shaanxi Province with an area of about $4 \times 10^6$ ha [1]. Pisha sandstone (PSS), also known as soft rock or feldspathic sandstone, is widely distributed throughout the region, covering more than $1.67 \times 10^6$ ha [2]. PSS is a distinct type of terrigenous clastic rock from the Mesozoic and Late Paleozoic periods (approximately 250 million years ago) and is composed of argillaceous sandstone, sand shale, and mudstone [3]. PSS exhibits a loosely bonded structure, minimal diagenesis, and relatively low compressive strength [4]. When dry, PSS is hard as a rock, but it disintegrates rapidly into mud when exposed to water [5]. Due to its limited usability and severe soil erosion, PSS is viewed by local residents as an environmental menace. Nevertheless, researchers have discovered that PSS has excellent hydrophilicity and expansibility, making it a natural water-retention agent and soil amendment [4,6]. Pisha sandstone is rich in clay–silt particles and montmorillonite, with large specific surface area, strong cation adsorption capacity, and outstanding colloidal properties, which promote the cementation and agglomeration of aeolian sandy soil in Mu Us Sandy Land [6–8]. Hence, researchers suggested using a combination of PSS and sandy soil to improve water retention ability and soil quality due to the complementary characters and structures of the two materials.

Incorporating PSS into sandy soil to create compound soils offers an effective approach for managing soil degradation and severe erosion, expanding arable land to support local agriculture and gradually establishing a new soil resource [7,9]. Several studies have demonstrated that the addition of PSS can significantly alter particle distribution and improve the texture of the compound soil [10,11]. Furthermore, the incorporation of PSS into sandy soil enhances its water and fertilizer retention capacity. Wang et al. (2013) reported a 2.7-fold increase in the water retention capacity of sandy land after PSS and sandy soil blending and that PSS is an effective measure to improve the water retention and fertilizer retention capacity of aeolian sandy soil, in which the volume ratio of PSS to aeolian sandy soil of 1:2 is the appropriate ratio [9]. As a soil amendment, PSS also contributes to the enhancement of the field soil organic matter (SOM) content, cation exchange capacity (CEC), and aggregate formation in sandy soil [7]. In practical applications, over 1600 ha of newly cultivated land resources have been established by incorporating PSS into sandy soils, and the addition of PSS has improved the utilization efficiency and productivity of aeolian sandy soil resources in Mu Us Sandy Land [9,12]. Despite extensive research efforts, the current focus is predominantly on macro aspects such as erosion resistance, hydraulic parameters, or productivity [11,13]. The microscopic particle interaction force mechanism underlying the impact of PSS addition on aggregate stability in compound soil remains incompletely understood.

The stability of aggregates is the primary and direct factor in assessing soil erosion and quality, as it is significantly affected by soil electrochemical properties and interaction forces among particles [14,15]. For example, Liu et al. (2020) demonstrated that inputting SOM changed electrochemical properties on the soil particle surface during vegetation succession, subsequently enhancing the van der Waals attraction between the particles and ultimately improving soil structure stability [16]. Similarly, Hu et al. (2021) observed that incorporating biochar as a soil amendment increased the CEC, specific surface area (SSA), and charge density of the soil surface, which significantly enhanced the molecular attraction, and weakened the repulsive force between soil particles and consequently improved aggregate stability [17]. Xu et al. (2015) reported that the release of small particles (<2 μm) from a compound soil sample (20% montmorillonite and 80% kaolinite) was four times higher than that of pure montmorillonite, indicating that the addition of fine particles could enhance soil

aggregate stability [15]. Moreover, the difference of surface potentials or kaolinite contents led to a difference in soil aggregate stability, highlighting that the influence of soil particle composition ratios on surface electrochemical properties and aggregate stability is critical. In conclusion, it is reasonable to infer that electrochemical properties and particle internal forces among compound soil (PSS and sandy soil) particles can be altered with the addition of PSS, further profoundly impacting soil aggregate stability. However, there have been limited studies to date on how PSS addition influences sandy soil particle interaction forces by changing particle surface properties and its impacts on aggregate stability in compound soil. Further investigations in this area are crucial for elucidating the mechanisms by which PSS stabilizes compound soil aggregates.

Therefore, in this study, we collected soil samples from a ten-year field experiment with varying application rates of PSS in sandy soil (PSS: sandy soil = 0:1, 1:5, 1:2, 1:1, and 1:0, $v/v$) to assess soil aggregate stability. The primary objective is to quantitatively investigate the impact of PSS addition on soil interaction forces (SIFs) and soil aggregate stability while also elucidating the underlying mechanisms of compound soil aggregate stability and compound soil erosion control in Mu Us Sandy Land. Our study will provide some theoretical references for further understanding of the compound soil structure improvement and sandy soil erosion control in Mu Us Sandy Land.

## 2. Materials and Methods

### *2.1. Experimental Site and Design*

The Pisha sandstone and sandy soil used in this study were obtained from Daji Han Village in Yuyang District, Yulin city, located within the Mu Us Sandy Land of China (109°28′ E, 38°27′ N) (Figure 1). Prior to field compounding, any remaining plant roots and boulders were removed from the samples. After natural drying, the samples were crushed and passed through a 5 mm sieve.

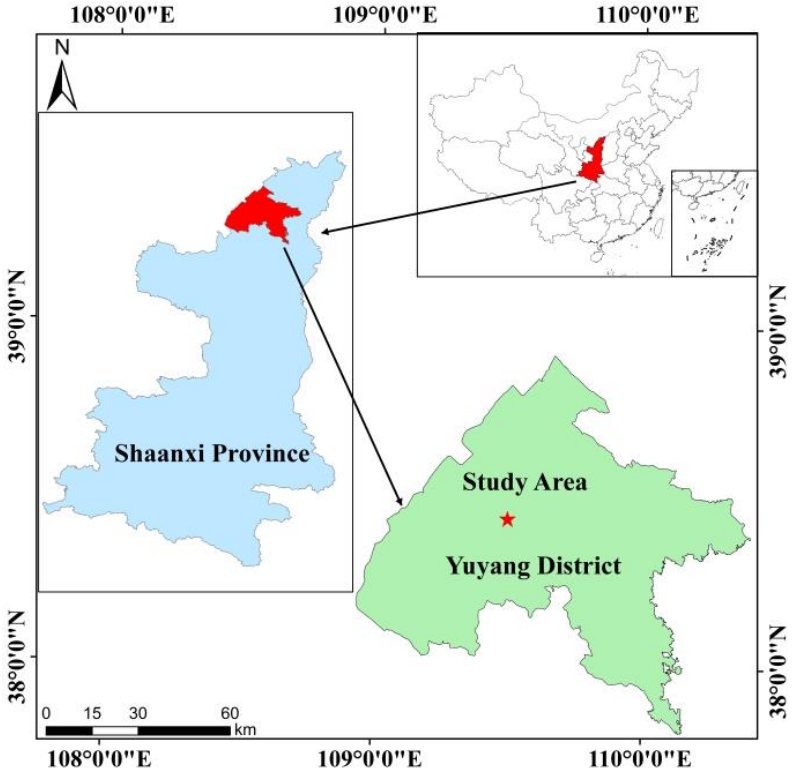


**Figure 1.** Location of the experimental site.

The field experiment was conducted in Fuping County (109°11′ E, 34°42′ N), Shaanxi Province, China. The area represents a typical semi-arid continental climate, and the mean

annual rainfall is 473 mm. Rainfall distribution during the year is highly uneven, with approximately 59% occurring from July to September. The potential annual evaporation is nearly 1300 mm, more than twice the amount of the rainfall. The field experimental plots (2 × 2 m) were filled 30 cm deep by compound soil consisting of five volume ratios of PSS and sandy soil (0:1, 1:5, 1:2, 1:1, and 1:0, *v*/*v*), and the electrochemical properties, particle interaction forces, and their effects on aggregate stability were studied for five compound soil samples with different volume ratios of Pisha sandstone and sandy soil. The objective is to determine the internal force control mechanism of the addition of PSS at different ratios to improve the structure and quality of aeolian sandy soil. Corn and wheat were cultivated on the compound soil for ten years. Each group was replicated three times.

### 2.2. Determination of the Basic Properties of the Compound Soil

The compound soil samples were collected randomly from three locations in each plot using a soil auger at a depth of 0–20 cm. The test materials were naturally dried, followed by the removal of stones and plant roots, and then sieved through a 2 mm mesh. The soil organic carbon (SOC) content was measured by the $K_2Cr_2O_7$ oxidation method [18]. Soil pH was determined by a pH meter with a soil to water ratio of 1:2.5 [19]. The carbonate content was determined using a gas volume method [20]. The primary clay minerals in compound soils were determined by X-ray diffraction analysis (Ultima IV, manufactured by Rigaku Corporation of Japan, Tokyo, Japan). The primary clay minerals in PSS were montmorillonite (~7%), hydromica (~10%), kaolinite (~12%), and chlorite (~11%), whereas the primary clay minerals in sandy soil were hydromica (~8%) and kaolinite (~6%). Soil particle size distributions were determined using the pipette method and were classified into sand (2–0.02 mm), silt (0.02–0.002 mm), and clay (<0.002 mm) based on the International Soil Texture Classification System. CEC and SSA were measured according to the method proposed by Li et al. (2013), involving the saturation of soil samples with hydrogen ions and conducting ion exchange experiments with a mixture of $Ca(OH)_2$ and NaOH. The concentrations of $Ca^{2+}$ and $Na^+$ were detected to calculate CEC, *SSA*, and surface charge density ($\sigma_0$) according to the double layer theory [21]. Specific procedures followed those in previous research [16]. The basic compound soil properties are presented in Table 1.

**Table 1.** Basic physicochemical properties and surface electrochemical properties of compound soils under different compound ratios.

| v (PSS):v (SS) | Particle Size Distribution | | | pH | $CaCO_3$ ($g \cdot kg^{-1}$) | SOC ($g \cdot kg^{-1}$) | CEC ($cmol \cdot kg^{-1}$) | *SSA* ($m^{2.5} \cdot g^{-1}$) |
|---|---|---|---|---|---|---|---|---|
| | Sand (%) | Silt (%) | Clay (%) | | | | | |
| 0:1 | 93.8 ± 0.25 a | 2.33 ± 0.21 d | 3.87 ± 0.22 a | 8.39 ± 0.01 b | 29.14 ± 2.49 d | 3.28 ± 1.13 cd | 4.68 ± 0.04 d | 2.54 ± 0.31 d |
| 1:5 | 88.15 ± 0.52 b | 8.85 ± 0.71 c | 3.00 ± 0.19 a | 8.78 ± 0.05 a | 40.84 ± 1.76 c | 4.50 ± 0.86 bc | 6.45 ± 0.07 c | 7.47 ± 2.12 cd |
| 1:2 | 82.82 ± 2.13 c | 12.94 ± 1.74 b | 4.24 ± 1.7 a | 8.75 ± 0.06 a | 44.59 ± 1.95 c | 5.24 ± 0.52 ab | 6.67 ± 0.08 c | 10.96 ± 0.77 c |
| 1:1 | 83.29 ± 0.61 c | 14.13 ± 1.37 b | 2.58 ± 0.82 a | 8.72 ± 0.02 a | 55.09 ± 2.26 b | 6.59 ± 0.52 a | 13.76 ± 0.22 b | 28.71 ± 3.84 b |
| 1:0 | 64.18 ± 1.81 d | 31.59 ± 1.86 a | 4.23 ± 0.07 a | 8.21 ± 0.10 c | 144.66 ± 5.16 a | 2.22 ± 0.52 cd | 17.91 ± 0.18 a | 37.24 ± 4.90 a |

Notes: v (PSS):v (SS) represents the combined treatment of the volume ratio of Pisha sandstone to sandy soil; SOC, soil organic carbon; CEC, cation exchange capacity; *SSA*: specific surface area. Different lowercase letters for the same index are significantly different at the 0.05 level ($p < 0.05$); Values are means ± standard deviation ($n = 3$).

### 2.3. Determination of Soil Surface Charge Properties

Compound soil surface charge properties include cation exchange capacity (CEC), specific surface area (SSA), surface charge density ($\sigma_0$), surface electric field strength (E), and surface potential ($\varphi_0$). These parameters were determined according to the combined method for the determination of soil surface properties [22]. The detailed steps were as follows. Firstly, due to the high content of $CaCO_3$ in soft rock, it was necessary to decalcify the soil samples. Briefly, differently treated crushed (<0.25 mm) samples were decalcified by washing with 0.5 mol $L^{-1}$ HCl solution three times until no $CO_2$ was released in the suspension. Secondly, $H^+$-saturated samples were prepared by washing approximately 100 g soil four times with 500 mL of 0.1 mol $L^{-1}$ HCl and then with deionized water

repeatedly until the solution was free of $Cl^{-1}$ in the suspension. The $H^+$-saturated soil samples were obtained, oven-dried at 60 °C, and sieved through a 0.25 mm sieve. Thirdly, certain amounts of $H^+$-saturated samples were weighed into 150 mL triangular bottles, and equal volumes (approximately 55 mL) of 0.01 mol $L^{-1}$ $Ca(OH)_2$ and NaOH solution were added. Because pH affects the soil surface charge properties, after 24 h of shaking, the pH values of the differently treated suspension were adjusted to 7.0 with 1 mol $L^{-1}$ HCl solution. The quantities of $Ca^{2+}$ and $Na^+$ absorbed on soil particles were determined by measuring the activities and concentrations of $Ca^{2+}$ and $Na^+$ in the supernatants using a flame photometer and an atomic absorption spectrometer, respectively.

Finally, the electrochemical properties of compound soil were calculated by introducing the measured data into the following Equations (1)–(5) [22,23].

$$\varphi_0 = \frac{2RT}{2(\beta_{Ca} - \beta_{Na})F} \ln \frac{\alpha^0_{Ca} N_{Na}}{\alpha^0_{Na} N_{Ca}} \tag{1}$$

$$\sigma_0 = \mathrm{sgn}(\varphi_0) \sqrt{\frac{\varepsilon RT}{2\pi} \left( \alpha^0_{Na} \exp \frac{\beta_{Na} F \varphi_0}{RT} + \alpha^0_{Ca} \exp \frac{2\beta_{Ca} F \varphi_0}{RT} \right)} \tag{2}$$

$$E = 4\pi\sigma_0/\varepsilon \tag{3}$$

$$SSA = \frac{N_{Na}\kappa}{m\alpha^0_{Na}} \exp \frac{\beta_{Na} F \varphi_0}{2RT} = \frac{N_{Ca}\kappa}{m\alpha^0_{Ca}} \exp \frac{\beta_{Ca} F \varphi_0}{RT} \tag{4}$$

$$CEC = 10^5 S\sigma/F \tag{5}$$

where $\varphi_0$ (mV) is the particle surface potential; $\sigma_0$ (C $m^{-2}$) is the surface charge density; $R$ (J $K^{-1}$ $mol^{-1}$) is the universal gas constant; $T$ (K) is the absolute temperature; $F$ (C $mol^{-1}$) is the Faraday constant; $E$ (V $m^{-1}$) is the surface electric field strength; $SSA$ ($m^2$ $g^{-1}$) is the specific surface area; $CEC$ (cmol $kg^{-1}$) is the cation exchange capacity; $Z$ is the charge of the cation; $\beta_{Na}$ and $\beta_{Ca}$ are the corresponding modification factors of $Z$ for $Na^+$ and $Ca^{2+}$, respectively; $\varepsilon$ is the dielectric constant for water ($8.9 \times 10^{-9}$ $C^2$ $J^{-1}m^{-1}$); $\kappa$ ($dm^{-1}$) is the Debye–Hückel parameter; $I$ (mol $L^{-1}$) is the ionic strength; $c^0{}_i$ (mol $L^{-1}$) is the equilibrium concentration of the cation (i = $Ca^{2+}$, $Na^+$) in the bulk solution; $\alpha^0{}_i$ (mol $L^{-1}$) is the activity of the cation (i = $Ca^{2+}$, $Na^+$) in the bulk solution; $N_i$ (mol $g^{-1}$) is the total number of cations (i = $Ca^{2+}$, $Na^+$) adsorbed on the soil particle surface.

In this experiment, the calculation equations of compound soil electric field intensity distribution with distance are as follows:

$$\varphi(x) = \frac{4RT}{F} \tan h^{-1} \left( ae^{-kx} \right) \tag{6}$$

$$a = \tan h \left( \frac{ZF\varphi_0}{4RT} \right) \tag{7}$$

$$E(x) = \sqrt{\frac{8\pi RT}{\varepsilon}} \left[ c_0 \left( e^{\frac{-ZF\varphi(x)}{RT}} - 1 \right) \right] \tag{8}$$

where $\varphi$(x) is the potential at x distance from the particle surface, V; $x$ is the distance between two adjacent particles in the double electric layer, nm; $a$ is the intermediate variable; $E$(x) is the electric field strength at x distance from the particle surface, V $m^{-1}$.

### *2.4. Quantification of Soil Particle Interaction Forces*

The compound soil particle interaction forces (SIFs) include electrostatic, van der Waals, and hydration forces. The net pressure ($P_{net}$) of the compound soil interaction force is the sum of the electrostatic repulsive pressure ($P_{ele}$), hydration pressure ($P_{hyd}$), and van der Waals force ($P_{vdW}$) in this experiment. Here, based on the determination

and calculation results of the surface charge properties of composite soils, the $P_{net}$ can be calculated according to the following equations [17,24]:

$$P_{net} = P_{ele} + P_{hyd} + P_{vdW} \quad (9)$$

$$P_{ele} = \frac{2}{101} RTc_0 \left\{ \cos h \left[ \frac{ZF\varphi(d/2)}{RT} \right] - 1 \right\} \quad (10)$$

$$P_{hyd} = 3.33 \times 10^4 exp^{-5.76 \times 10^9 d} \quad (11)$$

$$P_{vdW} = -\frac{A_{eff}}{0.6\pi} (10d)^{-3} \quad (12)$$

where R ($J \cdot K^{-1} \cdot mol^{-1}$) is the universal gas constant; T (K) represents absolute temperature; $c_0$ ($mol \cdot L^{-1}$) refers to the cation concentration of the equilibrium solution; Z is the cation valence; F ($C\ mol^{-1}$) is the Faraday constant; $A_{eff}$ (J) is the effective Hamaker constant, which is usually between $10^{-21}$ and $10^{-19}$ J [25] and can be calculated using the soil water characteristic curve [26,27]. As PSS and sandy soil are not real soils in the strict sense, the $A_{eff}$ for quartz [17,28] (main composition of sandy soil) instead of that for sandy soil was used, and the $A_{eff}$ of PSS was measured, while that of other compound soils was interpolated based on the mixing ratio. d (dm) represents the distance between two adjacent particles, while φ(d/2) (V) denotes the electric potential at the midpoint of the overlap region of their respective double layers.

### *2.5. Evaluation of Soil Aggregate Stability*

In this experiment, the aggregate breaking strength was utilized for assessing the aggregate stability to characterize the structural stability of compound soil aggregates [17,24]; this strength is defined as the percentage of particles (diameters < 10 and <5 μm). An increase in the percentage of fine particles indicates a decrease in soil aggregate stability. In this study, NaCl solutions with varying concentrations (1, $10^{-1}$, $10^{-2}$, $10^{-3}$, and $10^{-5}$ mol $L^{-1}$) were prepared in five cylinders (500 mL), and 20 g of 1–5 mm $Na^+$-saturated soil aggregate was slowly added to each cylinder (three replicates). Subsequently, the soil aggregate was submerged for 2 min, followed by careful inversion of the cylinders four times within the next 2 min. The mass percent of released particles (<10 and <5 μm) to total aggregate was determined using the pipette method according to Stokes law [28]. Throughout the experiment, strict adherence to proper techniques and precautions was maintained.

## 3. Results

### *3.1. Influences of PSS on Compound Soil Properties*

Table 1 presents the fundamental properties of different compound soils. As can be seen from this table, sandy soil had the highest sand content while PSS has less sand and more clay than sandy soil. With the addition of PSS, the silt content in the compound soil increased significantly, while the sand content decreased ($p < 0.05$). The pH of the compound soils was slightly higher compared to PSS and sandy soil. The incorporation of PSS led to a significant increase in the $CaCO_3$ content ($p < 0.05$), and the $CaCO_3$ content of the composite soil at the ratio of 1:1 was nearly twice that of the sandy soil. The initial SOC content in PSS was only 2.22 $g \cdot kg^{-1}$; however, the addition of PSS substantially elevated the SOC levels in the compound soils. After ten years of cultivation, among the various ratios tested, the SOC content was highest in the compound soil with a ratio of 1:1, approximately twice that of sandy soil and three times that of pure PSS. The organic matter content of PSS and sandy soil in the combined treatment at 1:5, 1:2, and 1:1 increased by 37.32%, 59.78%, and 101.07%, respectively, compared with the control treatment without PSS. Across the different proportions, the CEC ranged from 4.68 cmol $kg^{-1}$ to 17.91 cmol $kg^{-1}$, with an average of 9.89 cmol $kg^{-1}$. Furthermore, the SSA of the compound soil varied from 2.54 to 37.24 $m^2\ g^{-1}$, with an average of 17.38 $m^2\ g^{-1}$. Overall, the incorporation of PSS

significantly enhanced the CEC and SSA ($p < 0.05$), while the CEC value notably increased from 4.68 to 13.76 cmol·kg$^{-1}$ ($p < 0.05$).

### *3.2. Changes of Surface Potential and Electric Field Strength of Compound Soils*

The surface electric field intensity and internal force of compound soil particles are affected by the composition of soil electrolytes and the concentration of the electrolyte solution [29]. In general, with the increase in electrolyte concentration, the electric field strength and internal force between soil particles show a decreasing trend, and the net attraction between soil particles increases. It was found that with the increase in the distance between soil particles, the electrostatic repulsive force, van der Waals attractive force, and hydration repulsive force between compound soil particles will gradually decrease [30,31]. The surface potential of soil particles at different electrolyte concentrations can be calculated by Equation (1), and the results are shown in Table 2. Under the same electrolyte concentration, the soil surface potential (absolute value) decreased with the increase in the soft rock content. For all the compound soils, the surface potential (absolute value) decreased with the increase in the electrolyte concentration. Specifically, when the electrolyte concentration varied from $10^{-5}$ to 1 mol L$^{-1}$, the absolute value of the surface potential for the 1:5, 1:2, and 1:1 groups decreased by 290.6, 288.9, and 287.6 mV, respectively.

**Table 2.** Surface potentials of soil particles under different electrolyte concentrations and compound ratios.

| Electrolyte Concentration (mol·L$^{-1}$) | Compound Soil Surface Potential (mV) | | | | |
|---|---|---|---|---|---|
| | **0:1** | **1:5** | **1:2** | **1:1** | **1:0** |
| 1 | −470.3 | −431.4 | −413.4 | −401.2 | −401.4 |
| 0.1 | −352.2 | −313.3 | −295.4 | −283.2 | −283.4 |
| 0.01 | −293.2 | −254.6 | −236.9 | −224.8 | −225.0 |
| 0.001 | −234.7 | −196.7 | −179.4 | −167.7 | −167.9 |
| 0.00001 | −177.3 | −140.8 | −124.5 | −113.6 | −113.8 |

The electric field distribution curves around soil particles under different electrolyte concentrations can be further obtained based on the surface potential values and Equations (6)–(8). As shown in Figure 2, the electric field intensity decreased with the increase in the distance between particles. Similarly, the increase in electrolyte concentration also led to the reduction of the electric field intensity around soil particles, and the variation range of the surface electric field was sharply reduced. For example, the electric field action distance was only within 10 nm when the electrolyte concentration was 1 mol L$^{-1}$; however, with the dilution of the electrolyte concentration to $10^{-5}$ mol L$^{-1}$, the range of the electric field intensity increased rapidly, reaching more than 100 nm.

The electric field intensity values of the five compound soils at 10 nm and different concentrations are shown in Table 3. The electric field intensity gradually decreased with the addition of soft rock, while the difference of the electric field intensity of compound soils with the same concentration was small. However, for the same treatment, the change of electrolyte concentration resulted in an order of magnitude change in the electric field intensity. When the concentration was diluted from 1 to $10^{-2}$ mol L$^{-1}$, the intensity of the electric field jumped from double figures to $10^6$ orders of magnitude, but when the concentration decreased from $10^{-2}$ to $10^{-5}$ mol L$^{-1}$, the electric field intensity was still within the range of $10^6$ orders of magnitude. The above results indicate that an electrolyte concentration of $10^{-2}$ mol L$^{-1}$ was the key concentration that affected the electric field intensity in this study.

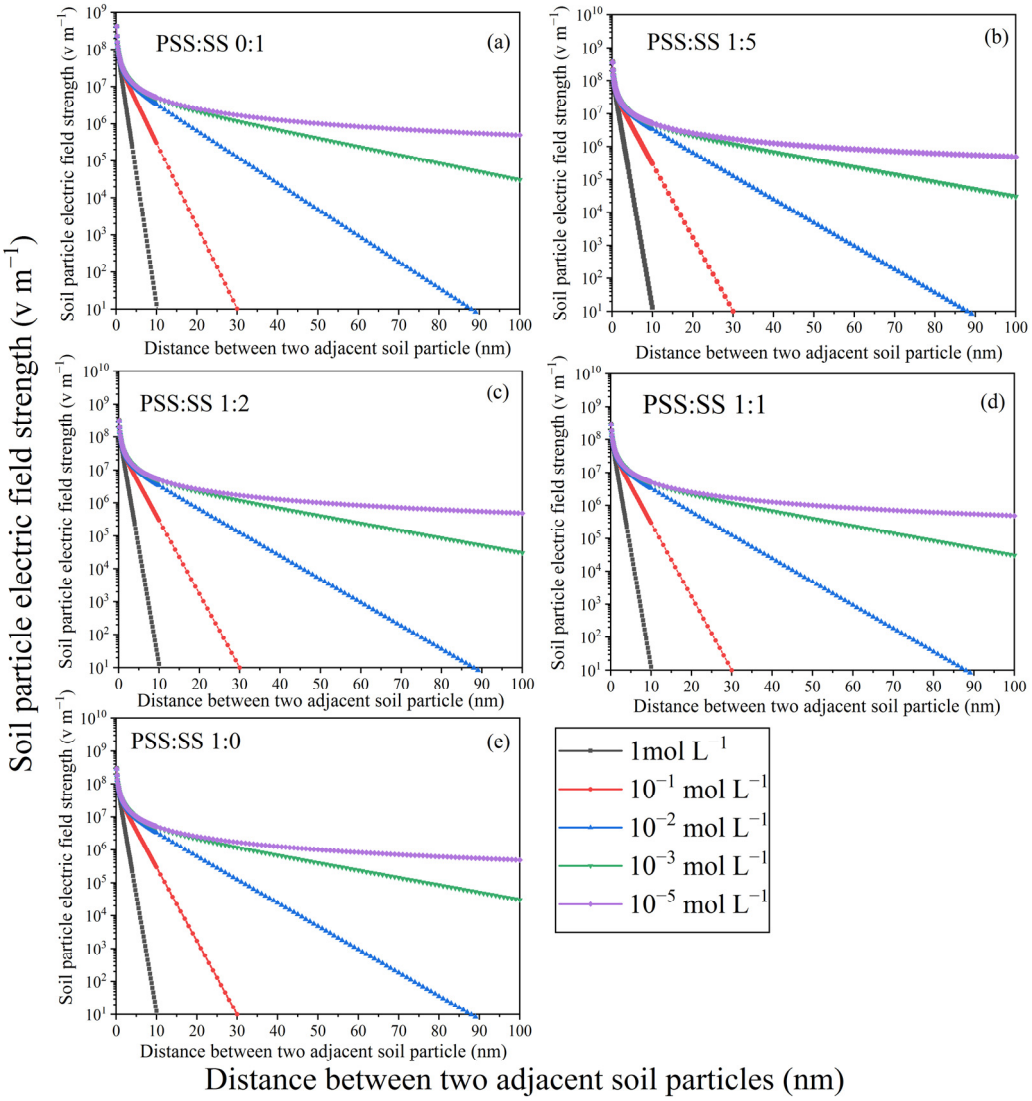


**Figure 2.** Distribution of compound soil electric field around soil particles under different electrolyte concentrations and compound ratios.

**Table 3.** Soil surface electric field strength at the distance of 10 nm from particle surfaces under different electrolyte concentrations and compound ratios.

| Electrolyte Concentration (mol·L$^{-1}$) | Compound Soil Electric Field Strength (−V m$^{-1}$) | | | | |
|---|---|---|---|---|---|
| | **0:1** | **1:5** | **1:2** | **1:1** | **1:0** |
| 1 | $5.12 \times 10^6$ | $5.11 \times 10^6$ | $5.10 \times 10^6$ | $5.09 \times 10^6$ | $5.09 \times 10^6$ |
| 0.1 | $4.90 \times 10^6$ | $4.89 \times 10^6$ | $4.88 \times 10^6$ | $4.87 \times 10^6$ | $4.87 \times 10^6$ |
| 0.01 | $3.40 \times 10^6$ | $3.39 \times 10^6$ | $3.38 \times 10^6$ | $3.37 \times 10^6$ | $3.37 \times 10^6$ |
| 0.001 | $3.04 \times 10^5$ | $3.00 \times 10^5$ | $2.98 \times 10^5$ | $2.96 \times 10^5$ | $2.96 \times 10^5$ |
| 0.00001 | 13.76 | 13.30 | 12.95 | 12.71 | 12.71 |

### *3.3. Changes in the Aggregate Stability of Compound Soils*

To investigate the effects of soil particle interaction forces on aggregate stability, the aggregate breaking strength of compound soils under different electrolyte concentrations is plotted in Figure 3. It can be seen that the aggregate breaking strength of compound soils followed the order of 1:0 > 1:1 > 0:1 > 1:5 > 1:2. It was observed that the breaking strength initially decreased followed by an increase in PSS under each electrolyte concentration. In other words, as the level of PSS amendment increased, the soil aggregate stability improved

initially, reaching its highest point at the 1:2 ratio, before gradually weakening. The addition of Pisha sandstone improved the structural stability and erosion resistance of the compound soil. Additionally, we discovered that a low electrolyte concentration resulted in greater breaking strength. Under the condition of a high concentration (1 mol $L^{-1}$) of electrolyte solution, almost no small particles were released or broken.

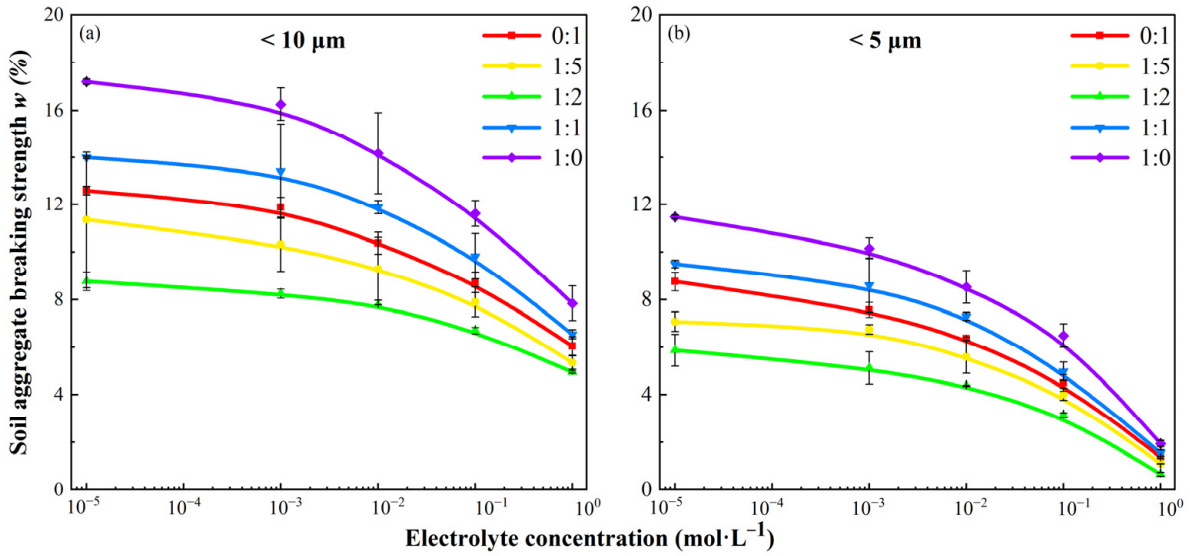


**Figure 3.** Changes in aggregate breaking strength under different electrolyte concentrations and compound ratios. Note: Error bars represents the standard deviation ($n$ = 3).

### *3.4. $P_{net}$ of Compound Soil Particles*

The net pressure between two adjacent particle surfaces is the sum of electrostatic repulsion, van der Waals attraction, and hydration repulsion, which was calculated according to Equations (9)–(12) (Figure 4). Generally speaking, Pisha sandstone is rich in montmorillonite and clay–silt particles; the addition of Pisha sandstone enhanced the van der Waals attraction force, reduced the net repulsive force between compound soil particles, and promoted the agglomeration of aeolian sandy soil. The overall trend of the net resultant force under different addition ratios of Pisha sandstone was 1:0 < 1:1 < 1:2 < 1:5 < 0:1. The negative value indicated that the compound soil particles were net attractive, which means that the addition of Pisha sandstone enhanced the agglomeration force and structural stability of compound soil particles. For example, when the concentration was 1 mol $L^{-1}$, the distance of the sites corresponding to zero net pressure gradually decreased with the increase in the soft rock. At a high electrolyte concentration of 1 mol $L^{-1}$, when the distance between adjacent soil particles of the compound soil was greater than 2.3 nm, except for the 0:1 treatment without the addition of PSS, the net pressure between soil particles under the other four compound soil treatments with the addition of PSS was negative, showing a net attraction. Recent studies have shown that when the distance between soil particles is less than 2 nm, the hydration repulsive force plays a leading role; meanwhile, the dry soil aggregates encounter water, the distance between particles extends to 1.5~2 nm by the hydration repulsion, and the soil aggregates expand only slightly [32]. When the distance between soil particles is greater than 2 nm, van der Waals attractive force and electrostatic repulsive force play a leading role, and the agglomeration or fragmentation of soil aggregates is affected by electrostatic repulsive force, van der Waals attractive force, and hydration repulsive force [32,33]. When two adjacent soil particles of compound soil were infinitely close together, at any electrolyte concentration, the net pressure of the five compound soils was always repulsive and could reach tens of thousands of atmospheres. For instance, at the ratio of 1:2 compound soil, the net repulsive pressure at the particle distance of 0.2 nm was about 10,700 atm at the electrolyte concentration of 1 mol $L^{-1}$. In

addition, when the electrolyte concentration was >$10^{-2}$ mol $L^{-1}$, the net pressure increased substantially with decreasing electrolyte concentration at the same distance. However, when the electrolyte concentration ≤ $10^{-2}$ mol $L^{-1}$, the net pressure distribution curves almost overlapped. Here in, taking the compound soil with the ratio of 1:1 as an example (at a distance of 2 nm), when the electrolyte concentration decreased from 1 to $10^{-2}$ mol $L^{-1}$, the increase in net pressure was 18.12 atm. However, when the concentration decreased from $10^{-2}$ to $10^{-5}$ mol $L^{-1}$, the net repulsive pressure increase was only 0.42 atm. These findings showed that $10^{-2}$ mol $L^{-1}$ was also the critical concentration affecting the net pressure of compound soil.

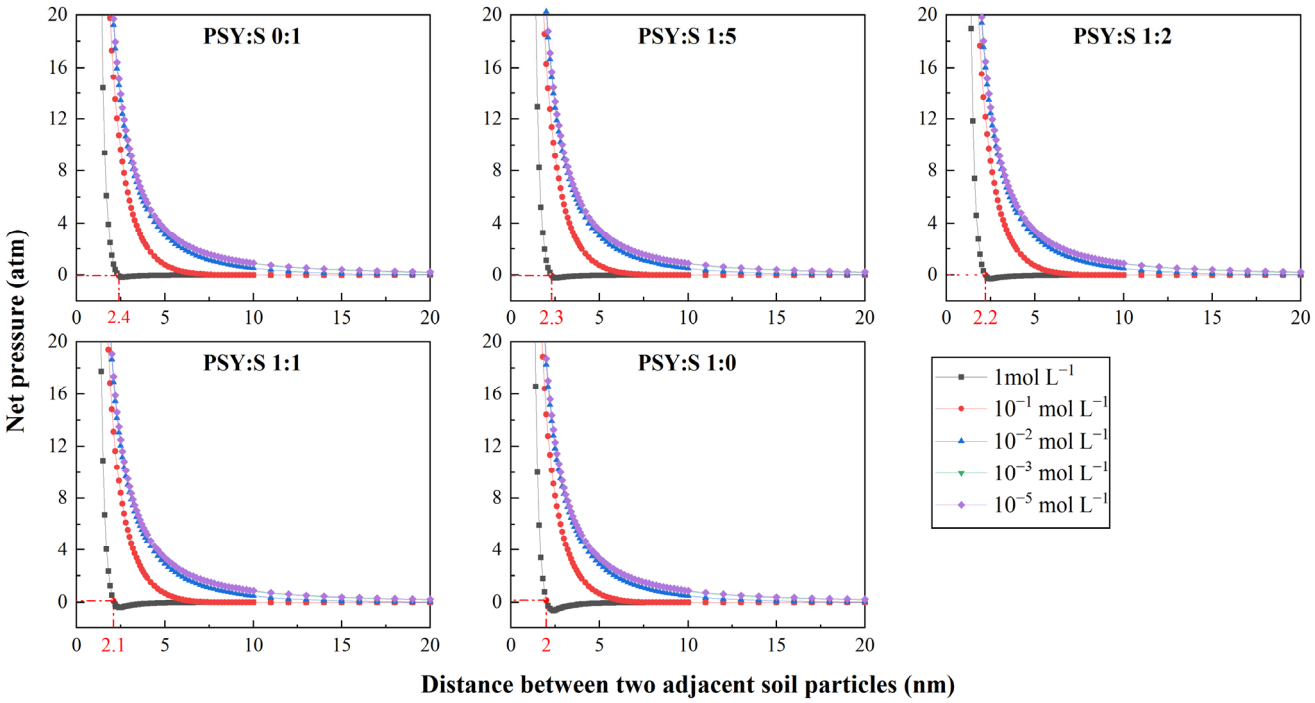


**Figure 4.** Distribution of net pressure ($P_{net}$) around compound soil particles at different electrolyte concentrations.

In order to further evaluate and analyze the influence of different compound ratios of Pisha sandstone and sandy soil on the variation of the net resultant force between compound soil particles, the distribution diagram of net resultant force at the distance of 2.0 nm and 2.4 nm between compound soil particles was drawn (Figure 5). The net resultant force between the compound soil particles under different compound ratios of Pisha sandstone and sandy soil showed a trend of 1:0 < 1:1 < 1:2 < 1:5 < 0:1. The smaller the net resultant value, the greater the net attraction between the compound soil particles. The research data showed that with the addition of Pisha sandstone, the smaller the net force between particles, the greater the net attraction. The combination of Pisha sandstone and sandy soil could promote the cementation and agglomeration of soil particles, and the net attraction between compound soil particles was enhanced. When the electrolyte concentration of the solution decreased from 1 mol $L^{-1}$ to $10^{-2}$ mol $L^{-1}$, the net resultant force between the composite soil particles increased rapidly under different compound ratios, and the attraction between the compound soil particles weakened sharply. When the electrolyte concentration of the solution decreased from $10^{-2}$ mol $L^{-1}$ to $10^{-5}$ mol $L^{-1}$, the net resultant force between the soil particles of the compound Pisha sandstone and sandy soil changed only slightly, and the change of the force between the compound soil particles tended to be gentle. The above results showed that the electrolyte concentration of $10^{-2}$ mol $L^{-1}$ was the key concentration threshold for the change of the interaction between Pisha sandstone and sandy soil in the compound soil. When the electrolyte concentration

of the solution was $10^0$ mol $L^{-1}$ and the particle distance of the compound soil was 2.4 nm, the net resultant force of the sandy soil without Pisha sandstone was 0.09 atm, and the net resultant force of the compound soil with Pisha sandstone added was negative under the four compound treatments (1:1, 1:2, 1:5, 0:1), and the particles were attractive. However, the aggregate stability of compound soil may be affected not only by the net resultant force between particles but also by the granulometric composition and addition ratios of the Pisha sandstone samples. In order to further clarify the influential factors of particle agglomeration of compound soil, the relationship between the net resultant force between compound soil particles and aggregate breaking strength will be further analyzed below.

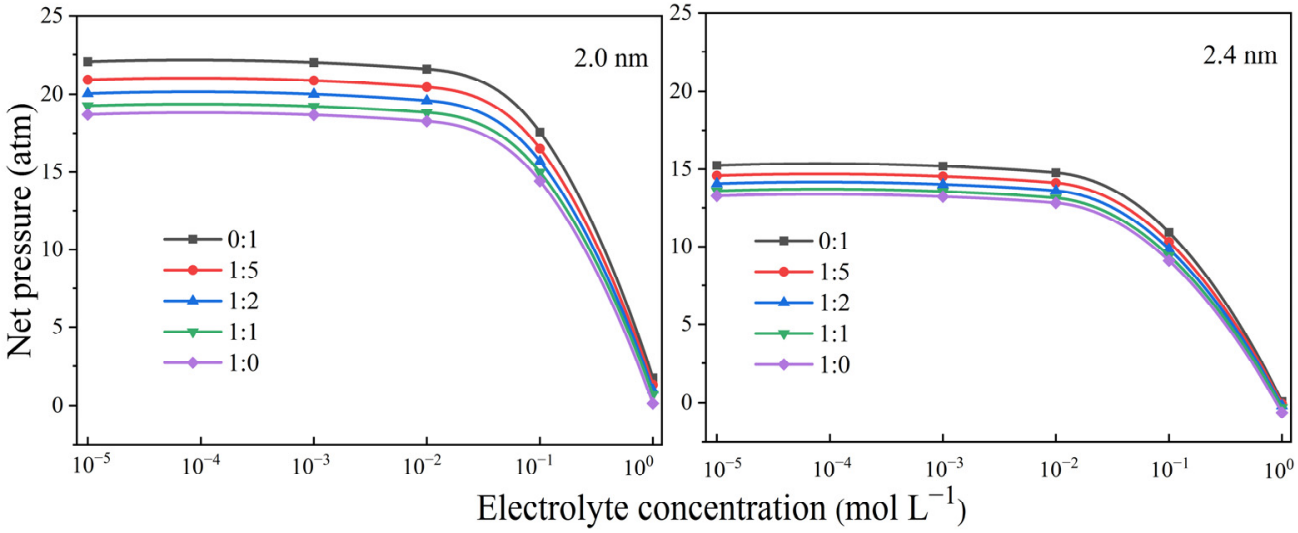


**Figure 5.** Net pressures at 2.0 nm and 2.4 nm distances between compound soil particles under different electrolyte concentrations and compound ratios.

### *3.5. Relationship between the Net Pressure ($P_{net}$) and the Aggregate Breaking Strength of under Different Compound Ratios*

To further quantitatively analyze the combined effects of compound soil particle interaction forces and the compound ratio on aggregate stability, we established the relationship between the net pressure at a 2 nm soil particle distance and the aggregate breaking strength of the compound soils (Figure 6). The five compound soil samples with different volume ratios of Pisha sandstone and sandy soil (0:1, 1:5, 1:2, 1:1, and 1:0, $v/v$) were used to study the compound soil particle interaction forces and their effects on aggregate stability. Herein, the compound soils were classified into two categories based on the different Pisha sandstone mixed ratios (50% Pisha sandstone). There was a significant positive exponential relationship between the aggregate breaking strength and the soil net pressures. This indicates that the soil aggregate stability decreased exponentially with the increase in the net pressure of soil particles. Different proportions of compound soil cannot directly establish the relationship between the internal force and aggregate breaking strength. It is necessary to classify the groups of different compound proportions. When $p < 0.05$, the $R^2$ values of fitting curve A and fitting curve B reached more than 0.7, which indicates that both force and particle composition had important effects on aggregate stability. For different compound soil samples, when the PSS content was below 50%, the stability of the aggregates was primarily influenced by SIFs between soil particles. Conversely, when the PSS content was 50% or higher, the stability of the aggregates was affected by both the fine particle content and soil interaction forces. The addition of different ratios of Pisha sandstone samples had different effects on the composition of the compound soil particles. Therefore, our results suggest that the aggregate stability of compound soils was not only affected by compound soil particle interaction forces but also by the granulometric composition and addition ratios of the Pisha sandstone samples.

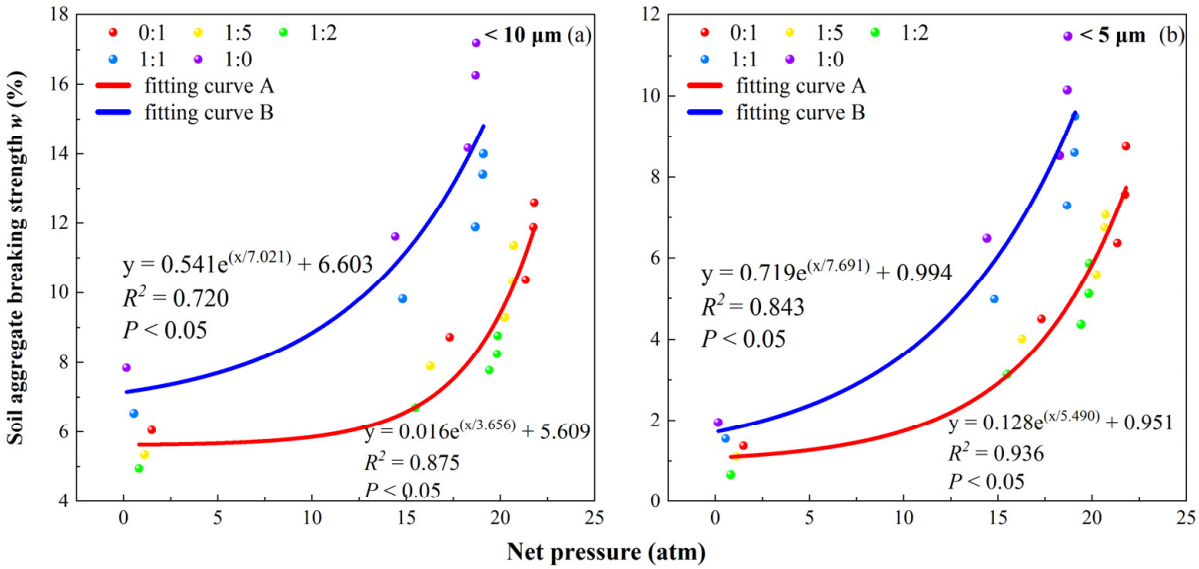


**Figure 6.** The relationship between the net pressure ($P_{net}$) and the aggregate breaking strength of compound soil under different compound ratios. Notes: Fitting curve A represents the compound soil group with PSS content < 50%. Fitting curve B represents the compound soil group with PSS content ≥ 50%.

## 4. Discussion

### *4.1. Responses of Compound Soil Properties to Soft Rock Addition*

The addition of PSS can alter the particle size distribution of compound soils. As the input of PSS increased, the silt content increased while the sand content decreased (Table 1). Existing research has also mentioned a comparable trend, where the soil texture improved and the distribution of soil grades tended to be better [11]. This is mainly because sandy soil has relatively coarse particles and a high sand content, while PSS contains clay and silt with a large specific surface area. When they are combined, the fine particles fill the large pores, converting non-capillary porosity into capillary porosity, reducing soil permeability and thereby improving the soil water-holding capacity and cation adsorption capacity [12]. Our results also demonstrate a progressive increase in the carbonate content with the addition of PSS, which aligns with previous studies by Guo et al., who showed that the addition of Pisha sandstone significantly increased the calcium carbonate content of aeolian sandy soil [34]. The PSS used in our study belongs to a calcareous PSS [9]. After compounding with sandy soils, the calcium carbonate content in compound soils significantly increased, promoting the aggregate formation of sandy soils due to cementation effects [35]. After ten years of tillage management, the SOC content of compound soils increased with increasing PSS application rates (Table 1). This is consistent with prior literature [7,36], which also found significantly higher fertility in compound soils with the addition of Pisha sandstone compared to sandy soil. This result can be explained as follows: on the one hand, the addition of PSS to sandy soil increased the presence of fine particles, and Ingelmo et al. (2003) indicated that the soil organic matter (SOM) tended to concentrate around these fine particles, allowing for the formation of more organic–inorganic complexes [37]. On the other hand, the change in particle composition led to a more uniform composite soil texture, increasing the ability to retain water and fertilizer. Additionally, the ten-year farming environment also increased amount of crop residue recovery and promoted the accumulation of organic matter [6,8,12].

Pisha sandstone was rich in clay–silt particles and montmorillonite, with a large specific surface area and strong cation adsorption capacity, which led to an increase in CEC and SSA with the addition of Pisha sandstone (Table 1). These findings are consistent with prior research, which reported that the addition of PSS significantly increased the ion adsorption capacity and CEC content of aeolian sandy soil [7,38]. The increase in CEC

can be attributed to the particle composition and mineral composition of the compound soil. Iturri and Buschiazzo (2014) reported that CEC is influenced by both the clay and silt content, while Hepper et al. (2006) showed that the changes in silt content positively affect CEC [39,40]. With the addition of PSS, the content of fine particles (<0.02 mm) increased in the compound soils (Table 1). PSS contains montmorillonite, which has the largest surface area and CEC among the minerals present [7,41]. In summary, the presence of fine particles and the montmorillonite content in Pisha sandstone play crucial roles in the substantial increase in CEC and SSA in aeolian sandy soil.

### *4.2. Effects of PSS Application on Soil Aggregate Stability and SIFs*

According to the relationship between $P_{net}$ and the aggregate breaking strength (Figures 3 and 4), the compound soils were classified into two categories based on the different mixing ratios (50% PSS). The aggregate breaking strength exhibited a significant positive exponential relationship with soil $P_{net}$. Therefore, our results suggest that the aggregate stability of compound soils was not only affected by SIFs but also by the granulometric composition and addition ratios of the Pisha sandstone samples. As mentioned earlier, the decrease in electrolyte concentration will lead to an increase in the net force, which in turn leads to an increase in the aggregate breaking strength and a decrease in the stability of the aggregates. The experimental results are consistent with the theoretical analysis, indicating that soil internal force is an important factor affecting the aggregate stability. Similar results are also mentioned in the literature by Hu et al. (2015) and Liu et al. (2021), who found that the electrolyte concentration of loess solution was positively correlated with the net attraction between particles [24,42]. The internal force between soil particles is closely related to the electrolyte concentration in solution, which is the key to the stability and fragmentation of the aggregate structure [32,43,44]. However, the aggregate breaking strength varies with the addition of soft rock, and the ratio of PSS to sandy soil was 1:2, which had the best effect on improving the structural stability of sandy soil aggregates. The experimental results are not consistent with the theoretical predictions, indicating that in addition to the internal force, the compound ratio and the granulometric composition of the Pisha sandstone samples are also important factors affecting the structure stability of the compound soil. Pisha sandstone is rich in montmorillonite and clay–silt particles with a large specific surface area.

Our results indicated that $P_{net}$ tended to decrease with increasing PSS content at any given concentration, whereas the experimental data of aggregate stability showed that the 1:2 group was the most stable combination, while the 1:0 group was the least stable among all groups (Figure 3). These results may be explained by differences in the particle size distribution of the compound soils. Methodically, according to previous research [23], strong repulsive forces mainly produce single grains and micro aggregates, while the maximum particle size measured when assessing the stability of aggregates by the pipette method was 10 μm in our study, which is lower than the minimum particle size of sand. Therefore, the method is very sensitive to the sand content. As indicated in the study of Liu et al. (2021), soil with a higher sand content exhibits lower aggregate breaking strength, which could cause soil aggregates to appear more stable [42]. Similarly, in our study, compound soils with ratios of 0:1, 1:5, and 1:2 had more than 50% sandy soil content, which may lead to better aggregate stability than those with less than 50% sandy soil, such as soils with compound ratios of 1:0 and 1:1. On the other hand, according to the research of Liu et al. (2021), the pipette method is greatly affected by the difference in particle composition [42]. The smaller particles in the soil will be released after the aggregates are broken, and the stability will decrease. This is the reason why the compound soil with a high PSS content had a high breaking strength, which is not conducive to soil erosion resistance and structure improvement. From a particle composition perspective, Xu et al. (2015) found that after montmorillonite and kaolinite were compounded in different proportions, the internal pore characteristics of the compound soil structure were different, so the rate of water entering the aggregates will be different, which will further lead to

different degrees of aggregate fragmentation and ultimately lead to differences in aggregate stability [15]. Therefore, these results suggest that both the SIFs and the particle composition may significantly influence the aggregate stability of compound soils.

## 5. Conclusions

In this study, we observed that the addition of PSS to sandy soil resulted in an increase in the $CaCO_3$ content and silt particle content, while the sand particle content decreased. Furthermore, a ten-year field study revealed that the incorporation of PSS led to an increase in SOM, CEC, and SSA. Calculations disclosed a decrease in repulsive forces and an increase in attractive force following PSS addition. The amendment of PSS caused an increase in the particle net attraction of compound soil, with an essential concentration ($10^{-2}$ mol $L^{-1}$) significantly impacting SIFs in compound soils. For different compound soil samples, when the PSS content was below 50%, the stability of aggregates was primarily influenced by SIFs between soil particles. Conversely, when the PSS content was 50% or higher, the stability of aggregates was affected by both the fine particle content and soil interaction forces. The PSS and sandy soil treatment with a ratio of 1:2 had a better effect on the particle interaction force and structural stability of compound soil. In summary, the aggregate stability of compound soils is influenced by both soil interaction forces and compound soil particle composition. The preliminary findings of this paper provide a quantitative description of the interaction forces in compound soils and provide a valuable scientific basis for PSS as a soil amendment to improve sandy soil quality and erosion protection resistance. Our research results will provide important theoretical support for soil and water conservation and ecological environment construction in Mu Us Sandy Land and a new path for soil structure improvement and erosion control in similar sandy land.

**Author Contributions:** Conceptualization, Z.L., L.Z. and Y.Z.; methodology, Z.L., J.H. and F.H.; software, Z.L. and L.Z.; writing—original draft preparation, Z.L., F.H. and L.Z.; writing—review and editing, Z.L., R.Z. and X.L.; funding acquisition, J.H., Y.Z. and Y.S. All authors have read and agreed to the published version of the manuscript.

**Funding:** This work was supported by the National Natural Science Foundation of China (42307429), the Technology Innovation Center for Land Engineering and Human Settlements, Shaanxi Land Engineering Construction Group Co., Ltd. and Xi'an Jiaotong University (2024WHZ0232), the Natural Science Basic Research Program of Shaanxi (2023-JC-QN-0343 and 2023-JC-QN-0360), and the Scientific Research Item of Shaanxi Provincial Land Engineering Construction Group (DJTD-2024-1 and DJTD-2022-5).

**Institutional Review Board Statement:** Not applicable.

**Informed Consent Statement:** Not applicable.

**Data Availability Statement:** The data presented in this study are available on request from the corresponding author.

**Acknowledgments:** The authors are grateful to the Technology Innovation Center for Land Engineering and Human Settlements by Shaanxi Land Engineering Construction Group Co., Ltd. and Xi'an Jiaotong University, School of Human Settlements and Civil Engineering, Xi'an Jiaotong University, and the Institute of Land Engineering and Technology, Shanxi Provincial Land Engineering Construction Group, Xi'an, China. Special thanks go to the anonymous reviewers for their constructive comments in improving this manuscript.

**Conflicts of Interest:** Authors Zhe Liu, Yang Zhang, Jichang Han, Yingying Sun, Ruiqing Zhang were employed by the company Shaanxi Provincial Land Engineering Construction Group Co., Ltd. The remaining authors declare that the research was conducted in the absence of any commercial or financial relationships that could be construed as a potential conflict of interest.

## References


1. Liang, P.; Yang, X.P. Landscape spatial patterns in the Maowusu (Mu Us) Sandy Land, northern China and their impact factors. *Catena* **2016**, *145*, 321–333. [CrossRef]
2. Wang, Y.C.; Wu, Y.H.; Kou, Q.; Min, D.A.; Chang, Y.Z.; Zhang, R.J. Definition of arsenic rock zone borderline and its classification. *Sci. Soil Water Conserv.* **2007**, *5*, 14–18.
3. Bazhenov, M.L.; Chauvin, A.; Audibert, M.; Levashova, N.M. Permian and Triassic paleomagnetism of the southwestern Tien Shan: Timing and mode of tectonic rotations. *Earth Planet. Sci. Lett.* **1993**, *118*, 195–212. [CrossRef]
4. Liang, Z.S.; Wu, Z.R.; Yao, W.Y.; Noori, M.; Yang, C.Q.; Xiao, P.Q.; Leng, Y.B.; Deng, L. Pisha sandstone: Causes, processes and erosion options for its control and prospects. *Int. Soil Water Conserv. Res.* **2019**, *7*, 1–8. [CrossRef]
5. Guo, J.; Shi, Y.C.; Wu, L.J. Gravity erosion and lithology in Pisha sandstone in southern Inner Mongolia. *J. Groundw. Sci. Eng.* **2015**, *3*, 45–58. [CrossRef]
6. Zhang, H.O.; Guo, Z.; Li, J.; Lu, Y.J.; Xu, Y. Improvement of aeolian sandy soil in Mu Us, China with soft montmorillonite clay stone. *Agron. J.* **2020**, *113*, 820–828. [CrossRef]
7. Guo, Z.; Hui, W.; Li, J.; Yan, J.; Zhang, H.; Wang, H. Effects of Soft Rock on Soil Properties and Bacterial Community in Mu us Sandy land, China. *PeerJ* **2022**, *10*, e13561. [CrossRef]
8. Zhang, J.; Guo, Z. Response of Soil Structure and Crop Yield to Soft Rock in Mu Us Sandy Land, China. *Sci. Rep.* **2022**, *12*, 876. [CrossRef] [PubMed]
9. Wang, N.; Xie, J.C.; Han, J.C. A Sand Control and Development Model in Sandy Land Based on Mixed Experiments of Arsenic Sandstone and Sand: A Case Study in Mu Us Sandy Land in China. *Chin. Geogr.* **2013**, *23*, 700–707. [CrossRef]
10. Guo, Z.; Han, J.C.; Xu, Y.; Lu, Y.J.; Li, J. The mineralization characteristics of organic carbon and particle composition analysis in reconstructed soil with different proportions of soft rock and sand. *PeerJ* **2019**, *7*, e7707. [CrossRef]
11. Sun, Y.; Zhang, N.; Yan, J.; Zhang, S. Effects of Soft Rock and Biochar Applications on Millet (*Setaria italica* L.) Crop Performance in Sandy Soil. *Agronomy* **2020**, *10*, 669. [CrossRef]
12. Li, Y.; Cao, Z.; Long, H.; Liu, Y.; Li, W. Dynamic analysis of ecological environment combined with land cover and NDVI changes and implications for sustainable urban–rural development: The case of Mu Us Sandy Land. *J. Clean. Prod.* **2017**, *142*, 697–715. [CrossRef]
13. Sun, Z. Effect of Soft Rock Amendment on Soil Moisture and Water Storage in Mu Us Sandy Land. *IOP Conf. Ser. Mater. Sci. Eng.* **2018**, *381*, 012044. [CrossRef]
14. Chorom, M.; Regasamy, P.; Murray, R. Clay dispersion as influenced by pH and net particle charge of sodic soils. *Soil Res.* **1994**, *32*, 1243–1252. [CrossRef]
15. Xu, C.Y.; Yu, Z.H.; Li, H. The coupling effects of electric field and clay mineralogy on clay aggregate stability. *J. Soils Sediments* **2015**, *5*, 1159–1168. [CrossRef]
16. Liu, J.F.; Wang, Z.L.; Hu, F.N.; Xu, C.Y.; Ma, R.T.; Zhao, S.W. Soil organic matter and silt contents determine soil particle surface electrochemical properties across a long-term natural restoration grassland. *Catena* **2020**, *190*, 104526. [CrossRef]
17. Hu, F.N.; Xu, C.Y.; Ma, R.T.; Tu, K.; Zhang, F.B. Biochar application driven change in soil internal forces improves aggregate stability: Based on a two-year field study. *Geoderma* **2021**, *403*, 115276. [CrossRef]
18. Tiessen, H.; Moir, J.O. Total and Organic Carbon. In *Soil Sampling and Methods of Analysis*; Carter, M.R., Ed.; CRC Press: Boca Raton, FL, USA, 1993; Volume 38, pp. 187–199.
19. Lu, K. *Analytical Methods of Soil and Agricultural Chemistry*; Scientific Research Publishing: Wuhan, China, 1999.
20. Lierop, W.V.; Mackenzie, A.F. Carbonate Determination in Organic Soils. *Can J. Soil Sci.* **1974**, *54*, 457–462. [CrossRef]
21. Li, S.; Li, H.; Xu, C.Y.; Huang, X.R.; Xie, D.T.; Ni, J.P. Particle Interaction Forces Induce Soil Particle Transport during Rainfall. *Soil Sci. Soc. Am. J.* **2013**, *77*, 1563–1571. [CrossRef]
22. Li, H.; Hou, J.; Liu, X.M.; Hou, J.; Liu, X.M.; Li, R.; Zhu, H.L.; Wu, L.S. Combined determination of specific surface area and surface charge properties of charged particles from a single experiment. *Soil. Sci. Soc. Am. J.* **2011**, *75*, 21–28. [CrossRef]
23. Bissonnais, Y.L. Aggregate stability and assessment of soil crustability and erodibility: I. Theory and methodology. *Eur. J. Soil Sci.* **1996**, *47*, 425–437. [CrossRef]
24. Yu, Z.H.; Li, H.; Liu, X.M.; Xu, C.Y.; Xiong, H.L. Influence of soil electric field on water movement in soil. *Soil Tillage Res.* **2016**, *155*, 263–270. [CrossRef]
25. Zhang, Y.K.; Tian, R.; Yang, S.S.; Guo, X.M.; Li, H. Toward an Approach for Determining the Hamaker Constant of Soft Materials Using Dynamic Light Scattering. *Colloids Surf. A Physicochem. Eng. Asp.* **2021**, *630*, 127604. [CrossRef]
26. Hamaker, H.C. The London—Van der Waals attraction between spherical particles. *Physica* **1937**, *4*, 1058–1072. [CrossRef]
27. Tuller, M.; Or, D. Water films and scaling of soil characteristic curves at low water contents. *Water Resour. Res.* **2005**, *41*, 319–335. [CrossRef]
28. Yu, Z.H.; Zhang, J.B.; Zhang, C.Z.; Xin, X.L.; Li, H. The coupling effects of soil organic matter and particle interaction forces on soil aggregate stability. *Soil Tillage Res.* **2017**, *174*, 251–260. [CrossRef]
29. Liu, Z.; Zhang, Y.; Sun, Y.; Han, J.; Hu, F.; Li, J.; Li, X. Effects of the Changes of Particle Surface Electric Field and Interaction Force on the Reclaimed Soil Aggregate Structural Stability under the Application of Different Soil Conditioners. *Agronomy* **2023**, *13*, 1866. [CrossRef]

30. Yu, Z.H.; Zheng, Y.Y.; Zhang, J.B.; Zhang, C.Z.; Ma, D.H.; Chen, L.; Cai, T.Y. Importance of soil interparticle forces and organic matter for aggregate stability in a temperate soil and a subtropical soil. *Geoderma* **2020**, *362*, 114088. [CrossRef]
31. Gong, Y.; Tian, R.; Li, H. Coupling effects of surface charges, adsorbed counterions and particle-size distribution on soil water infiltration and transport. *Eur. J. Soil Sci.* **2018**, *69*, 1008–1017. [CrossRef]
32. Hu, F.N.; Liu, J.F.; Xu, C.Y.; Du, W.; Yang, Z.H.; Liu, X.M.; Liu, G.; Zhao, S.W. Soil internal forces contribute more than raindrop impact force to rainfall splash erosion. *Geoderma* **2018**, *330*, 91–98. [CrossRef]
33. Calero, J.; Ontiveros-Ortega, A.; Aranda, V.; Plaza, I. Humic acid adsorption and its role in colloidal-scale aggregation determined with the zeta potential, surface free energy and the extended-DLVO theory. *Eur. J. Soil Sci.* **2017**, *68*, 491–503. [CrossRef]
34. Guo, Z.; Zhang, H.O.; Wang, H.Y. Soft rock increases the colloid content and crop yield in sandy soil. *Agron. J.* **2020**, *113*, 677–684. [CrossRef]
35. Pihlap, E.; Steffens, M.; Kgel-Knabner, I. Initial soil aggregate formation and stabilisation in soils developed from calcareous loess. *Geoderma* **2021**, *385*, 114854. [CrossRef]
36. Li, W.Y.; Guo, Z.; Li, J.; Han, J.C. Effects of different proportions of soft rock additions on organic carbon pool and bacterial community structure of sandy soil. *Sci. Rep.* **2021**, *11*, 4624. [CrossRef] [PubMed]
37. Ingelmo, F.; Albiach, R.; Gamon, S. Organic matter of a soil amended with composted sludges and affected by simulated processes of soil degradation. *WIT Trans. Ecol. Environ.* **2003**, *64*, 10.
38. Zhen, Q.; Zheng, J.Y.; He, H.H.; Han, F.P.; Zhang, X.C. Effects of Pisha sandstone content on solute transport in a sandy soil. *Chemosphere* **2016**, *144*, 2214–2220. [CrossRef] [PubMed]
39. Iturri, L.A.; Buschiazzo, D.E. Cation exchange capacity and mineralogy of loess soils with different amounts of volcanic ashes. *Catena* **2014**, *121*, 81–87. [CrossRef]
40. Hepper, E.N.; Buschiazzo, D.E.; Hevia, G.G.; Urioste, A.; Antón, L. Clay mineralogy, cation exchange capacity and specific surface area of loess soils with different volcanic ash contents. *Geoderma* **2006**, *135*, 216–223. [CrossRef]
41. Yukselen-Aksoy, Y.; Kaya, A. Method dependency of relationships between specific surface area and soil physicochemical properties. *Appl Clay Sci.* **2010**, *50*, 182–190. [CrossRef]
42. Liu, J.F.; Hu, F.N.; Xu, C.Y.; Wang, Z.L.; Ma, R.T.; Zhao, S.W.; Liu, G. Comparison of different methods for assessing effects of soil interparticle forces on aggregate stability. *Geoderma* **2021**, *385*, 114834. [CrossRef]
43. Feng, B.; Li, Y.L.; Li, R.; Li, H. Error analysis in calculation and interpretation of AFM tip-surface interaction forces. *Adv. Colloid Interface Sci.* **2022**, *306*, 102710. [CrossRef] [PubMed]
44. Holthusen, D.; Reeb, D.; Horn, R. Influence of potassium fertilization, water and salt stress, and their interference on rheological soil parameters in planted containers. *Soil Tillage Res.* **2012**, *125*, 72–79. [CrossRef]